Eurasian Chem.-Technol. J. 27 (2026) 83–92
The journal of the Institute of Combustion Problems https://ect-journal.kz

https://doi.org/10.18321/ectj1685

Computational Assessment of Pharmacological, Toxicological, and Electronic Properties of Ephedrine Derivatives

Maxim Gubenko[1,2], Assel Ten[1], Elmira Yergaliyeva[2]*, Valery Dembitsky[3], Valentina Yu[1]

[1]A.B. Bekturov Institute of Chemical Sciences, 106 Sh. Ualikhanov St., Almaty 050010, Kazakhstan
[2]Akhmet Baitursynuly Kostanay Regional University, 47 Baytursynov St., Kostanay 110000, Kazakhstan
[3]N.D. Zelinsky Institute of Organic Chemistry, 47 Leninsky Prospekt, Moscow 119991, Russia

Article info

Received:
10 October 2025

Received in revised form:
19 December 2025

Accepted:
18 February 2026

Keywords:
Ephedrine
ADMET
PASS prediction
Spasmolytic activity
Analeptic properties

Abstract

Ephedrine and its derivatives have long been recognized for their therapeutic potential in the treatment of hypotension, asthma, and obesity. However, their use is limited by significant side effects, including cardiovascular risks and toxicity. This study presents a comprehensive computational evaluation of 13 ephedrine derivatives using integrated ADMET analysis, PASS prediction, and quantum-chemical approaches. Pharmacological profiles, toxicity risks, and electronic properties were systematically analyzed to establish structure–activity relationships. Key physicochemical parameters, pharmacokinetic properties, and toxicity risks were analyzed to identify compounds with optimal drug-like characteristics. The results highlight compound **5** as the most promising candidate, demonstrating high drug-likeness (Quantitative Estimate of Drug-likeness, QED = 0.85) and favorable pharmacokinetic properties. Conversely, compounds **3**, **11–13** exhibit high toxicity and require structural optimization. PASS predictions indicate diverse biological activities, including spasmolytic and analeptic effects, with compounds **5–7** showing significant potential for further development and compound **13** exhibiting antioxidant activity. DFT analysis of ephedrine, cephedrine and key derivatives (compounds **5, 7**, **13**) revealed an optimal HOMO-LUMO range (ΔE = 4.7–5.0 eV) for compounds with high activity and low toxicity, where derivative **5** exhibits the best balance. This study underscores the importance of rational drug design in optimizing therapeutic efficacy while minimizing adverse effects and environmental risks.

1. Introduction

Ephedra, commonly known as “ma huang” in Traditional Chinese Medicine (TCM), is one of the oldest medicinal plants used in traditional therapeutic systems. *Ephedra sinica*, a member of the Ephedraceae family, has been used in China for over 5,000 years [1–3]. While its traditional use is attributed to Emperor Shen Nung (ca. 3200 BC), documentation of its stimulant and antiasthmatic effects emerged during the Han Dynasty (ca. 207 BC–220 AD) [4–6]. Similarly, *Ephedra gerardiana* has a long history in Indian folk medicine. The herb was also known in Roman times but faded from European historical records during the medieval period [7–9].

L-Ephedrine is commonly used in pharmaceuticals as a decongestant and an antiasthmatic agent [10]. A key intermediate in its synthesis, l-phenylacetylcarbinol (l-PAC), can be obtained from Ephedra plants, through chemical resolution of racemic mixtures, or via biotransformation of benzaldehyde using yeast [11, 12]. Ephedrine and pseudoephedrine are among the earliest agents used to treat nasal congestion, primarily due to their vasoconstrictive effects on the nasal mucosa [13, 14].

*Corresponding author.
E-mail address: hooook1961@gmail.com

Ephedrine and its structural analogues have played a central role in pharmaceutical research due to their analeptic and antispasmodic effects, supporting their use in treating hypotension, asthma, and obesity [15, 16]. As a sympathomimetic amine, ephedrine activates both α- and β-adrenergic receptors, producing increases in blood pressure, heart rate, and bronchodilation [17, 18]. Despite these benefits, its use is limited by adverse cardiovascular effects, including tachycardia, arrhythmias, and elevated myocardial oxygen demand, posing significant risks in patients with heart disease [19, 20].

Prolonged ephedrine use may cause tachyphylaxis from norepinephrine depletion, hepatotoxicity, and ephedrine-containing urinary stones [21]. These risks have prompted the search for safer analogues. One such compound, cephedrine, developed at the Bekturov Institute of Chemical Sciences (Kazakhstan), includes a cyanoethyl group distinguishing it from ephedrine. Cephedrine acts as an antidepressant and psychostimulant with minimal anticholinergic activity and no MAO inhibition, reducing the likelihood of drug and food interactions [22–24].

Structural modifications like those in cephedrine (Scheme 1) demonstrate the potential for enhancing efficacy while minimizing side effects. Advances in computational methods, including QSAR/QSPR and virtual screening, support the discovery of new analogues with better receptor selectivity and safety profiles. These tools are essential for refining synthetic ephedrine derivatives into viable therapeutic agents.

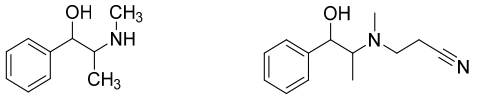

Scheme 1. Ephedrine and cephedrine.

This study focuses on developing structure–activity relationships (SAR) for ephedrine analogues using DFT/B3LYP-based quantum chemical analysis alongside ADMET and PASS computational pharmacology. The goal is to link frontier orbital properties with pharmacological effects and toxicity risks to support the design of safer, more effective compounds.

2. Materials and methods

The study investigated 13 compounds, including ephedrine (**1**), its derivatives, and synthetic analogues. Their chemical structures are presented in Scheme 2.

The pharmacokinetic and toxicological properties of the studied compounds were predicted using the ADMETlab 3.0 online platform. The predictions are based on QSAR/QSPR models trained on experimental datasets, including parameters related to drug absorption, distribution, metabolism, excretion, and toxicity. Calculations were performed using molecular descriptors automatically generated from the structural formulas of the compounds.

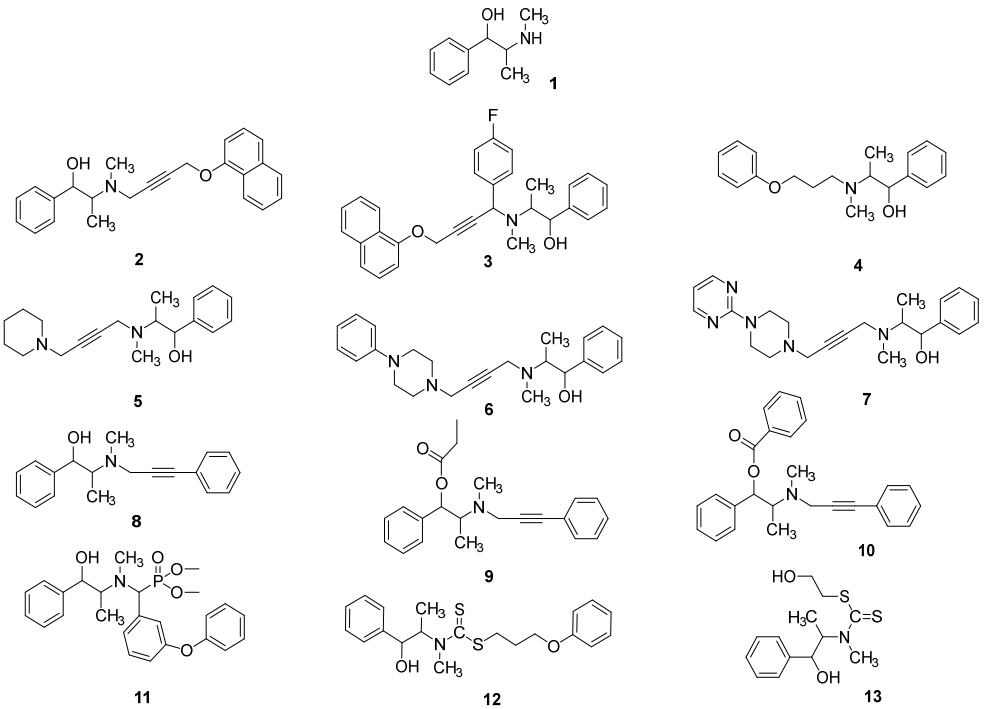

Scheme 2. Chemical structures of compounds 1–13.

Physicochemical properties (logP, logD7.4, TPSA, solubility), permeability parameters (Caco-2), plasma protein binding (PPB), volume of distribution (VDss), blood-brain barrier (BBB) penetration, metabolic interactions with cytochrome P450 isoenzymes (CYP3A4, CYP2D6, CYP2C19), and toxicological parameters, including hERG blockade, drug-induced liver injury (DILI), genotoxicity, and carcinogenicity, were assessed. Structural filters for toxophore fragments were additionally applied.

Prediction of the biological activity spectrum was performed using the PASS (Prediction of Activity Spectra for Substances) program. The method is based on Bayesian structure-activity relationship analysis using a training set of compounds with known pharmacological effects. For each activity, the probabilities of occurrence (P_a) and absence (P_i) were calculated. Activities with $P_a > 0.75$ were considered as potentially significant.

Quantum chemical calculations for ephedrine (**1**), cephedrine, and derivatives (**5, 7, 13**) were performed using density functional theory (DFT) with the B3LYP hybrid functional and the 6-311++G(d,p) basis set. Geometry optimization was performed without constraints in the gas phase. The correctness of the determined stationary points was confirmed by frequency analysis: the absence of imaginary frequencies indicated that true minima had been reached on the potential energy surface.

Based on the optimized structures, the energies of the frontier molecular orbitals (E_{HOMO} and E_{LUMO}), the energy gap ΔE ($E_{LUMO} - E_{HOMO}$), and global reaction descriptors in the Kuhn–Parak approximation were calculated: electronegativity (χ), chemical hardness (η), and electrophilicity index (ω). Calculations were performed using the Gaussian 16 package.

The obtained parameters were used for a comparative analysis of the reactivity of the compounds and to establish correlations between the electronic structure, predicted biological activity and toxicological characteristics.

3. Results and Discussion

3.1 ADME prediction

Physicochemical properties are essential for evaluating a compound's drug-likeness, influencing bioavailability, solubility, permeability, and metabolic stability. Radar plots generated via ADMETlab 3.0 (Fig. 1) depict the oral bioavailability profiles of compounds **1, 5, 7**, and **13** – identified as the most promising based on drug-likeness criteria. The blue zone outlines the acceptable range for oral drugs, while the green core represents lower-value ranges. The yellow shape reflects the calculated values for each compound, and its alignment within the purple region indicates compliance with oral drug-likeness benchmarks. Key therapeutic parameters of compounds **1–13** are presented in Table 1. Full datasets are provided in the Supplementary materials.

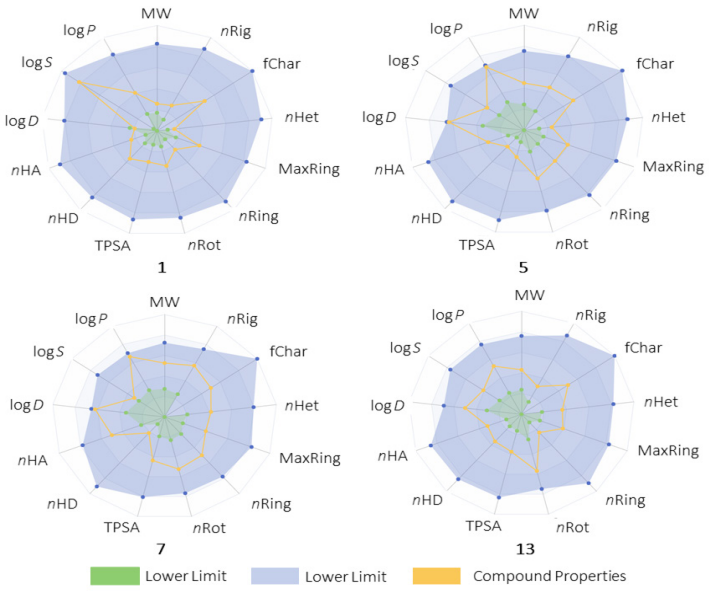

Fig. 1. Radar diagram of compounds **1, 5, 7, 13**. MW: molecular weight; *n*Rig: number of rigid bonds; fChar: formal charge; *n*Het: number of heteroatoms; MaxRing: number of atoms in the largest ring; *n*Ring: number of rings; *n*Rot: number of rotatable bonds; TPSA: topological polar surface area (Å^2); *n*HD: number of hydrogen bond donors; *n*HA: number of hydrogen bond acceptors; log *D*: logarithm of the octanol–water partition coefficient at physiological pH 7.4; log *S*: logarithm of aqueous solubility (mol·L^{-1}); and log *P*: logarithm of the octanol–water partition coefficient.

Table 1. Key properties for therapeutic significance and pharmacokinetics of **1–13** according to ADMETlab-3.0.

Property	QED	Fsp^3	Lipinski Rule	Pfizer Rule	GSK Rule	Golden Triangle	Reactive Compounds	Promiscuous Compounds
1	0.71	0.40	+	+	+	-	0.21	0.55
2	0.67	0.25	+	-	-	+	0.01	0.04
3	0.34	0.20	+	-	-	+	0.01	0.00
4	0.76	0.37	+	-	+	+	0.03	0.15
5	0.85	0.58	+	+	+	+	0.00	0.01
6	0.78	0.42	+	-	+	+	0.00	0.15
7	0.77	0.46	+	+	+	+	0.00	0.02
8	0.87	0.26	+	-	+	+	0.03	0.05
9	0.59	0.32	+	-	-	+	0.01	0.06
10	0.45	0.19	+	-	-	+	0.07	0.02
11	0.38	0.28	+	-	-	+	0.07	0.00
12	0.54	0.35	+	-	-	+	0.01	0.00
13	0.81	0.46	+	+	+	+	0.03	0.00

The QED score assesses drug-likeness based on structural features. Compounds **8** (0.87), **5** (0.85), and **13** (0.81) showed the highest values, indicating strong potential for therapeutic application [25].

The Fsp^3 metric, which measures carbon saturation, influences rigidity and target binding. Compound **13** (0.46) exhibited optimal rigidity, while compound **3** (0.2) showed increased flexibility, potentially reducing specificity [26].

All compounds **1–13** comply with Lipinski's Rule of Five [27]. The Pfizer rule filters out toxic or poorly absorbed compounds – only **1, 5, 7**, and **13** qualify. The GSK rule flags low-likelihood candidates – compounds **2, 3**, and **9–12** show limitations. The Golden Triangle criterion highlights the balance between size and lipophilicity – compound **1** fails this test [28]. Promiscuity risk is an indicator of off-target toxicity. Compound **1** scored high (0.55), suggesting a risk of side effects, while compounds **3, 5, 7, 10, 11, 12**, and **13** showed lower risks. Table 2 presents key ADME parameters for all compounds, enabling an integrated evaluation of bioavailability, metabolism, and safety to prioritize the most promising candidates.

Table 2. Absorption, distribution, metabolism and excretion characteristics of compounds **1–13** according to ADMETlab-3.0.

Property	Compound												
	1	**2**	**3**	**4**	**5**	**6**	**7**	**8**	**9**	**10**	**11**	**12**	**13**
Caco-2 Permeability (cm/s)	-5.0	-4.9	-5.2	-4.8	-4.9	-4.9	-5.0	-4.8	-4.6	-4.7	-5.0	-5.2	-5.1
PPB (%)	29.5	97.7	98.7	67.0	91.0	94.0	96.0	86.0	93.7	98.1	97.6	97.3	67.9
VDss (L/kg)	0.57	0.33	0.46	0.65	0.18	0.27	0.30	0.51	0.13	0.19	0.08	0.36	0.07
BBB	--	--	--	++	+++	+++	+++	+++	+++	+++	--	+	-
HLMS	+++	+++	+++	+++	+++	+++	+	-	+++	+++	+	+++	+++
CLplasma (mL/min/kg)	5.58	5.66	4.59	8.22	6.90	5.57	3.97	6.41	5.60	3.55	3.25	7.17	7.26
T1/2 (h)	4.63	1.89	0.63	2.88	2.80	1.80	1.36	2.38	0.94	1.13	1.56	0.35	0.98
CYP3A4 Inhib.	---	-	---	---	---	---	+++	++	+++	-	---	+++	--
CYP2D6 Inhib.	++	+++	+++	+++	+++	+++	+++	+++	+	-	-	+++	+
CYP2C19 Inhib.	---	+++	+++	---	---	--	-	---	-	+++	+++	+++	-
Transport Protein Inhibitor	+++	++	+++	++	-	-	++	-	---	++	+++	+++	+++

The ADME profile of compounds **1–13** highlights compounds **4, 5, 9,** and **13** as leading candidates. Their Caco-2 permeability scores (−4.78 to −4.59) exceed the −5.15 threshold for acceptable intestinal absorption [29].

Compounds **4** and **13** exhibit moderate plasma protein binding (~67%), suggesting sufficient free drug availability. Although compound **9** has high PPB (93.70%), its high permeability compensates for this.

Most compounds show good microsomal stability, though compounds **3** and **12** have short half-lives (0.63 h and 0.35 h), which may require frequent administration [30].

Compounds **2, 3**, and **10** show excessively high PPB (>97%), possibly reducing free drug levels. Low VDss in compounds **5, 9–11**, and **13** suggests limited tissue distribution [31].

Cytochrome P450 interactions are significant. Most compounds affect CYP2D6 and CYP3A4, increasing the risk of metabolic interactions. Compound **13** is a weak CYP2D6 inhibitor but is a CYP3A4/CYP2C19 substrate. Compound **7** shows similar interaction trends.

Transport protein inhibition varies; compounds **1, 3**, and **11–13** strongly inhibit multiple transporters (+++), increasing hepatotoxicity risk.

Overall, comprehensive ADME analysis supports prioritizing compounds with favorable permeability, moderate PPB, metabolic stability, and minimal transporter or enzyme inhibition. These features inform safer, more effective drug design.

3.2 Toxicity prediction

Table 3 contains the results of prediction of toxicological and ecological properties of compounds **1–13** based on toxicophore rules. Toxicophores are specific structural or chemical features of molecules that may be associated with undesirable biological effects.

Toxicological profiling of compounds **1–13** revealed key structural alerts linked to genotoxicity, mutagenicity, and skin sensitization. Compounds **2**, **3, 6, 7, 11–13** show violations in genotoxic/mutagenic filters, with **11–13** representing the highest risk. Skin sensitization is most pronounced in compounds **9**, **12**, and **13**, each with three violations, potentially limiting their topical use. Non-biodegradability is noted for all compounds except compound **1**, raising environmental concerns. Additionally, compounds **3, 12**, and **13** violate aquatic toxicity criteria, indicating potential ecological hazards.

FAF-Drugs4 flags extensive structural issues, especially for compound **6**, while SureChEMBL highlights compounds **11–13** for further toxicology testing. Table 4 summarizes compound-specific risks across key endpoints: neurotoxicity, hepatotoxicity, carcinogenicity, irritation, and cytotoxicity. Data is presented both as binary values and probabilities, categorized by risk level (low: 0–0.3, medium: 0.3–0.7, high: 0.7–1.0) and expressed qualitatively (+, ++, +++). This aids in selecting lead candidates and guiding structure-based refinement.

The most toxic compounds are **12** and **13**. For example, compound **12** has high values of drug-induced liver injury (DILI, 0.901), skin sensitization (0.851), carcinogenicity (0.926) and others. Compound **13** also shows high values of DILI (0.942), skin sensitization (0.969), carcinogenicity (0.719), eye irritation (0.853).

Table 3. Evaluation of toxicological and ecological properties of compounds **1–13** based on toxicophore rules according to ADMETlab-3.0.

Property	Compound												
	1	**2**	**3**	**4**	**5**	**6**	**7**	**8**	**9**	**10**	**11**	**12**	**13**
Aquatic Toxicity Rule	0	0	1	0	0	0	0	0	0	0	0	1	1
Genotoxic Carcinogenicity Mutagenicity Rule	0	1	1	0	0	1	1	0	0	0	2	1	1
NonGenotoxic Carcinogenicity Rule	0	0	1	0	0	0	0	0	0	0	0	2	2
Skin Sensitization Rule	0	1	1	0	0	0	0	1	3	2	0	3	3
Acute Toxicity Rule	0	0	0	0	0	1	0	0	0	0	0	0	0
Non-Biodegradable	0	1	2	1	1	1	1	1	1	1	1	1	1
SureChEMBL Rule	0	0	0	0	0	0	0	0	0	0	1	4	4
FAF-Drugs4 Rule	0	4	4	0	4	5	4	4	4	4	0	3	3

Table 4. Prediction of toxicological risks and ecological properties for compounds **1–13** using ADMETlab 3.0.

Property	Compound												
	1	**2**	**3**	**4**	**5**	**6**	**7**	**8**	**9**	**10**	**11**	**12**	**13**
hERG Blockers	0	+	+	++	++	+++	++	+	+	+	+	+	0
hERG Blockers (10 μM)	++	++	++	+++	++	+++	++	++	++	+++	++	++	+
DILI	0	0	0	+	0	0	+	0	+	+	++	+++	+++
AMES Toxicity	0	+	+	+	0	0	0	+	++	+	+	+	++
Rat Oral Acute Toxicity	+	+	+	+	++	++	++	+	++	+	+	+	+
FDAMDD	+++	+++	+++	+	+++	+++	+++	+++	++	++	++	0	0
Skin Sensitization	0	+	0	+	+++	++	++	+++	+++	+++	+	+++	+++
Carcinogenicity	0	+	++	++	0	0	0	+	+	+	++	+++	++
Eye Corrosion	0	0	0	0	+	0	0	+	+	0	0	0	+
Eye Irritation	0	+	+	+	+	0	0	+	+	+	++	+	+++
Respiratory	++	+++	++	+	+++	+++	+++	++	+	+	++	0	+
Human Hepatotoxicity	0	++	++	+	++	++	+++	++	+++	0	+	+	+
Drug-induced Nephrotoxicity	+	++	+++	+	++	+++	+++	++	++	+	+++	++	+
Drug-induced Neurotoxicity	++	++	+++	++	+++	+++	+++	++	++	++	++	+	+
Ototoxicity	++	++	+++	+	++	++	+	+	+	0	0	++	++
Hematotoxicity	0	0	0	0	0	0	+	0	+	0	+	0	0
Genotoxicity	+++	++	++	0	0	+++	+++	+	+	0	+++	+	+++
RPMI-8226 Immunitoxicity	0	0	0	0	0	0	0	0	0	0	0	0	0
A549 Cytotoxicity	0	0	+	+	0	0	0	0	+	+	0	0	+
HEK293 Cytotoxicity	0	+	++	+	+	++	+	+	++	++	0	++	+
BCF[a]	0.24	1.90	2.51	1.57	0.70	1.21	0.30	1.50	1.26	1.74	1.84	1.53	0.31
IGC_{50}[b]	2.53	4.21	4.22	3.69	3.23	3.47	2.83	3.76	3.88	4.55	3.87	4.15	2.90
$LC_{50}DM$[b]	3.72	5.52	6.38	4.74	4.63	4.54	4.14	4.85	5.07	5.91	5.72	5.64	4.37
$LC_{50}FM$[b]	2.84	4.95	5.66	4.26	3.94	4.09	3.31	4.35	4.64	5.52	4.75	5.07	3.38

[a] – log10(L/kg); [b] – log10[(mg/L)/(1000*MW)]

Compound **1** demonstrates the lowest toxicity for most parameters. It also exhibits the lowest values for BCF (0.24), IGC_{50} (2.53), $LC_{50}FM$ (2.84), and $LC_{50}DM$ (3.72). Compound **7** is also considered relatively safe (BCF = 0.3; IGC_{50} = 2.83; $LC_{50}DM$ = 4.14; $LC_{50}FM$ = 3.31). These data indicate its low bioaccumulation potential and minimal toxicity to aquatic organisms. The BCF (Bioconcentration Factor) parameter reflects the ability of a chemical to accumulate in the tissues of living organisms, while next values characterize toxicity to various model organisms: IGC_{50} – concentration of the test chemical in water in mg/L that causes 50% growth inhibition to *Tetrahymena pyriformis* after 48 h, $LC_{50}FM$ – concentration that causes 50% of fathead minnow to die after 96 h, and $LC_{50}DM$ – concentration that causes 50% of aquatic crustaceans Daphnia magna to die after 48 hours.

Compound **3** has a high BCF (2.51) and $LC_{50}DM$ (6.38), indicating a significant potential for bioaccumulation and increased toxicity for Daphnia magna. This makes it less safe in terms of impact on ecosystems. Compound **10** also stands out with high IGC_{50} (4.55) and $LC_{50}FM$ (5.52) values, indicating its high toxicity for *Tetrahymena pyriformis* and fish. Such characteristics highlight the significant risk of exposure of aquatic organisms to this compound.

The remaining compounds occupy an intermediate position in toxicity, demonstrating moderate values for all parameters.

Compound optimization should be aimed at reducing toxicity, improving pharmacokinetics and reducing environmental risks. This requires modifying the structure of molecules to reduce hERG channel blockade, hepatotoxicity, genotoxicity and other specific risks such as nephrotoxicity and neurotoxicity. It is important to optimize the ADME profile and reduce ecotoxicity by decreasing bioconcentration and optimizing IGC_{50}, $LC_{50}DM$ and $LC_{50}FM$ values. The use of *in silico* methods, *in vitro* and *in vivo* experiments will help confirm the safety and efficacy of compounds.

Analysis of the prediction results showed that compounds **1–13** generally do not activate key toxicological pathways such as NR-AhR, NR-AR, NR-PPAR-gamma, and others. However, some compounds demonstrate significant activity against NR-ER and SR-MMP.

Activation of the estrogen receptor (NR-ER) plays an important role in regulating the expression of genes associated with reproductive function, bone metabolism, and the cardiovascular system. Compounds **1, 8,** and **12** are highly active, making them potentially interesting for further study in the context of modulating estrogen-dependent processes. Compounds **2, 3, 6, 10**, and **11** also exhibit activity.

Matrix metalloproteinases (MMPs) play a key role in tissue remodeling, wound healing, and the progression of diseases such as cancer and arthritis. Activation or inhibition of MMPs can significantly affect extracellular matrix degradation. Only compound **10** exhibited moderate activity against SR-MMP, which may be due to its unique structure that facilitates interaction with matrix metalloproteinases.

3.3 PASS prediction

The structure–activity relationship (SAR) analysis of compounds **1–13,** derived from ephedrine, highlights the significant impact of specific molecular modifications on their predicted biological properties, as assessed by PASS (Prediction of Activity Spectra for Substances). Ephedrine serves as the reference compound, with structural changes such as functional group substitution or conformational alterations influencing both the probability of activity (P_a) and inactivity (P_i). These modifications can either enhance existing pharmacological effects or introduce novel activities, emphasizing the value of rational design in drug discovery.

Compound **1** demonstrates a strong potential for cardiovascular analeptic activity (P_a = 0.944, P_i = 0.002), and shows predicted inhibition of methylamine-glutamate N-methyltransferase (P_a = 0.88) and antagonism at α6β3β4α5 nicotinic receptors (P_a = 0.851). These effects appear to be unique to its core ephedrine scaffold, as derivative compounds show reduced or absent activity in these areas, suggesting that receptor interaction depends on precise molecular conformation.

Compound **2** acts as a CYP2C12 substrate (P_a = 0.872) and exhibits antispasmodic (P_a = 0.847) and membrane integrity agonist (P_a = 0.758) properties, suggesting cytoprotective potential.

The high predicted antispasmodic activity of compounds **4–7** suggests their potential for use in conditions associated with smooth muscle spasms, including gastrointestinal and urinary tract diseases, and bronchial obstructive disorders. Compared to the parent ephedrine, a number of derivatives demonstrate comparable or enhanced activity with improved drug-like properties, making them potentially more balanced candidates for further optimization.

Analeptic activity is retained in compounds **4, 5,** and **8** (P_a values ranging from 0.758 to 0.869), aligning with ephedrine's known stimulatory effects (P_a = 0.879), though this activity tends to diminish with further structural changes. This highlights the importance of preserving the parent scaffold, particularly the aromatic ring and amino group, to maintain CNS stimulatory effects.

Other notable activities include urological antispasmodic action in compound **6** (P_a = 0.775) and nootropic effects in compound **7** (P_a = 0.777), indicating potential for cognitive enhancement. The predicted nootropic activity of compound **7** indicates its potential for the treatment of cognitive impairment, including early stages of neurodegenerative diseases and mild cognitive impairment. Importantly, this activity is combined with a relatively favorable ADMET profile and the absence of genotoxicity, which is crucial for the development of drugs affecting the central nervous system.

Compound **8** is predicted as a CYP2D16 substrate (P_a = 0.837), suggesting its role in xenobiotic metabolism. Compounds **9–11** function as CYP2H substrates, while compound **12** is metabolized by flavin-containing monooxygenase (P_a = 0.88), both relevant to oxidative and metabolic pathways.

Compound **13** is predicted to inhibit arylacetonitrilase (P_a = 0.883) and NADPH peroxidase (P_a = 0.782), which may be associated with potential antioxidant-related effects. The presence of specific

substituents in its structure likely contributes to this distinct biological profile, highlighting the impact of targeted structural modifications on functional activity. The predicted modulation of oxidative pathways may be relevant in pathological conditions associated with oxidative stress, including neurodegenerative disorders, cardiovascular diseases, and chronic inflammatory processes. However, the concurrently predicted high toxicity profile suggests that further structural optimization would be required to reduce potential safety risks while preserving the therapeutically relevant properties of the compound.

Compound **3**, however, shows weak predictions, likely due to structural novelty, underrepresentation in PASS training data, or the presence of multiple conflicting functional groups. Its low scores may also reflect potential toxicity or limited bioavailability, necessitating experimental validation to clarify its biological potential.

3.4 HOMO-LUMO analysis

The presented data of DFT calculations (B3LYP/6-311++G(d,p)) allow a comparative analysis of the electronic properties of ephedrine, cephedrine and the most interesting derivatives **5** (favorable pharmacological profile), **7** (nootropic properties, low toxicity) and **13** (antioxidant properties; unique enzyme inhibition). The calculation results are shown in Table 5. Figure 2 shows an energy diagram with energy gap values and a visualization of frontier molecular orbitals.

All analyzed compounds demonstrate nucleophilic character, with notable variations in electronic properties influencing their predicted biological activity and safety profiles.

Ephedrine (compound **1**) and cephedrine possess the highest HOMO-LUMO energy gaps (ΔE > 5.5 eV), indicative of greater molecular stability and lower

Table 5. Quantum-chemical parameters of ephedrine derivatives calculated by DFT/B3LYP/6-311++G(d,p) method.

Property	Compounds				
	Ephedrine (1)	Cephedrine	5	7	13
HOMO energy (eV)	-6.11	-6.49	-5.69	-5.91	-5.99
LUMO energy (eV)	-0.53	-0.74	-0.73	-1.14	-1.13
ΔE gap (eV)	5.58	5.75	4.96	4.77	4.86
Electronegativity (χ, eV)	3.32	3.62	3.21	3.53	3.56
Chemical hardness (η, eV)	2.79	2.88	2.48	2.39	2.43
Electrophilicity (ω, eV)	1.98	2.28	2.07	2.60	2.61

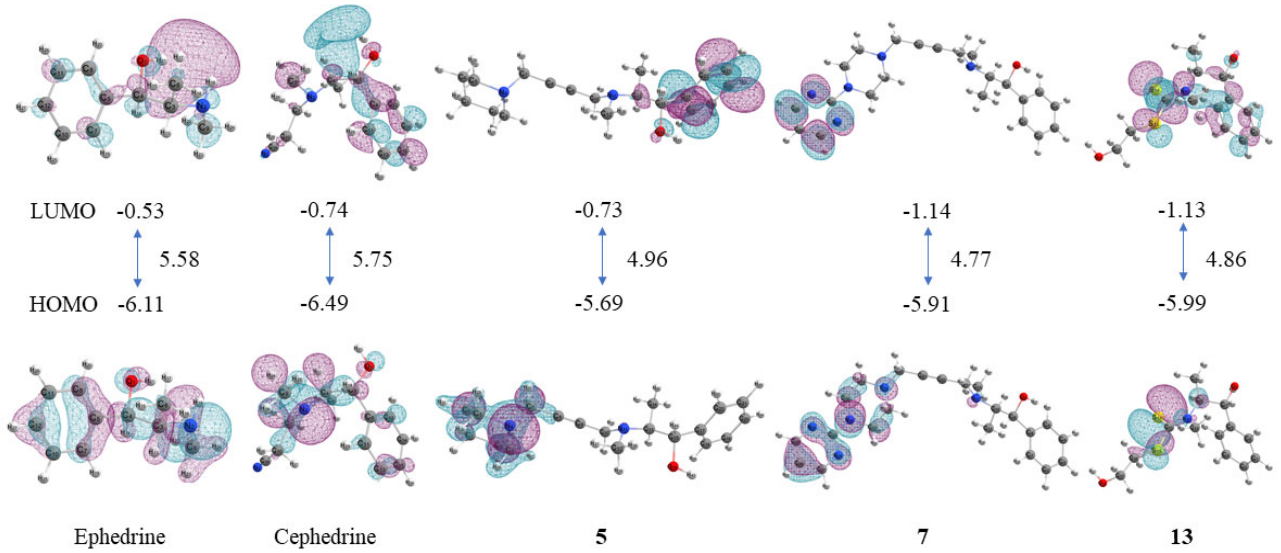

Fig. 2. Frontier molecular orbitals (HOMO and LUMO) of ephedrine, cephedrine, and compounds **5, 7,** and **13** calculated at the DFT/B3LYP/6-311++G(d,p) level of theory (isovalue = 0.02).

chemical reactivity. In contrast, compound **7** displays the smallest energy gap (ΔE = 4.77 eV), correlating with enhanced reactivity and a greater potential for electronic interactions with biological targets, as supported by PASS predictions. Its high electrophilicity index (ω = 2.6 eV) suggests a strong tendency to interact with electron-rich sites in biomolecules.

Compound **5** presents an intermediate ΔE value (4.96 eV), reflecting a balanced reactivity profile. This corresponds with its moderate biological activity, low toxicity, and reduced likelihood of non-specific interactions, further supported by its low electrophilicity (ω = 2.07 eV) [32].

Compound **13** shows a contradictory profile: it possesses high enzyme inhibitory potential – particularly toward NADPH peroxidase and arylacetonitrilase – attributed to its low LUMO energy (-1.13 eV) and elevated electrophilicity (ω = 2.61 eV). However, it is also associated with significant toxicity risks, including hepatotoxicity, nephrotoxicity (DILI+++), and carcinogenicity. This suggests a need for structural optimization, particularly modification of electron-withdrawing groups, to reduce ω and associated risks while preserving therapeutic enzyme-targeting properties. A study links the localization of HOMO on the hydroxyl group with antioxidant properties, which is confirmed by the PASS results in the case of compound **13**.

4. Conclusion

Combining PASS predictions, ADMETlab-3.0 profiles, and DFT calculations revealed structure–activity–toxicity relationships among 13 ephedrine-based compounds. Compound **5** is the top candidate, with high QED (0.85), excellent ADME profile, and strong spasmolytic activity (P_a = 0.975). However, its moderate hERG liability indicates the need for safety-driven optimization. Compounds **4–7** show high spasmolytic potential (P_a > 0.89) and good metabolic stability. Compound **7**, in particular, combines low promiscuity (0.02) and no genotoxicity, but its high PPB (96%) and low VDss (0.30 L/kg) may limit efficacy in tissues. Compound **13**, while offering notable antioxidant and enzyme-inhibitory effects, is a substrate for multiple CYP450 isoforms and poses high toxicity risks (e.g., DILI+++), requiring further evaluation. Quantum chemical data align with these findings: compounds with ΔE ~4.7–5.0 eV (e.g., **5** and **7**) tend to be active, while low LUMO values (< -1.1 eV, as in **13**) link to toxicity. Lowering electrophilicity (ω < 2.3 eV) may improve safety without compromising activity. The importance of combining rational structural modification with subsequent biological evaluation has been demonstrated in studies on ephedra alkaloids and related nitrogen-containing pharmacophores [9, 16, 33]. In this context, the present computational findings provide a foundation for further targeted synthesis and experimental validation of compounds with favorable activity and moderate toxicity to refine lead optimization.

Supporting Material

Supplementary data for this article, including ADMETlab 3.0 and PASS prediction results for compounds **1–13**, as well as graphical representations of HOMO and LUMO orbitals, are available online at: https://doi.org/10.18321/ectj1685

Acknowledgments

The study was carried out with the financial support of the Science Committee of the Ministry of Science and Higher Education of the Republic of Kazakhstan (grant No. AP23484420).

References

[1]. K.K. Chen, C.F. Schmidt, The action and clinical use of ephedrine, *J. Am. Pharm. Assoc.* 15 (1926) 836–842. DOI: 10.1001/jama.1926.02680110036011

[2]. A.S. Dousari, N. Satarzadeh, B. Amirheidari, et al., Medicinal and therapeutic properties of ephedra, *Rev. Bras. Farmacogn.* 32 (2022) 883–899. DOI: 10.1007/s43450-022-00304-3

[3]. W.A. Wannes, M.S. Tounsi, Phytochemicals, traditional uses, biological effects, and possible molecular mechanisms of Ephedra alata, *Future Integr. Med.* 2 (2023) 189–199. DOI: 10.14218/FIM.2023.00022

[4]. D. Bensky, A. Gamble, Chinese Herbal Medicine: Materia Medica, Eastland Press, Seattle, WA, 1993, p. 1305.

[5]. Y. Ding, E. Brand, W. Wang, et al., Licorice: Resources, applications in ancient and modern times, *J. Ethnopharmacol.* 298 (2022) 115594. DOI: 10.1016/j.jep.2022.115594

[6]. C. Ai, Y. Zou, H. Liu, et al., Traditional Chinese herbal medicine for allergic diseases: a review, *Am. J. Chin. Med.* 51 (2023) 779–806. DOI: 10.1142/S0192415X23500374

[7]. D. Jones, Ephedra (Ma-huang); Today and Yesterday: Traditional and Topical Aspects of its Nutritional and Clinical Applications, In: Proceedings of AHPA Ephedra International Symposium, Arlington, VA, December 1999.

[8]. S. Choudhary, H. Kaurav, G. Chaudhary, Medicinal importance of Ephedra gerardiana in Ayurveda and modern sciences, *Asian J. Pharm. Pharmacol.* 7 (2021) 110–117. DOI: 10.31024/ajpp.2021.7.3.1

[9]. S. Tang, J. Ren, L. Kong, et al., Ephedrae herba: A review of its phytochemistry, pharmacology, clinical application, and alkaloid toxicity, *Molecules* 28 (2023) 663. DOI: 10.3390/molecules28020663

[10]. C.M. Tripathi, S.C. Agarwal, S.K. Basu, Production of L-phenylacetylcarbinol by fermentation, *J. Ferment. Bioeng.* 84 (1997) 487–492. DOI: 10.1016/S0922-338X(97)81900-9

[11]. J.O. Westman, P. Ylitervo, C.J. Franzén, et al., Effects of encapsulation of microorganisms on product formation during microbial fermentations, *Appl. Microbiol. Biotechnol.* 96 (2012) 1441–1454. DOI: 10.1007/s00253-012-4517-y

[12]. N.D. Fabricant, Effect of progressively buffered solution of ephedrine on nasal mucosa, *J. Am. Med. Assoc.* 151 (1953) 21–25. DOI: 10.1001/jama.151.1.21

[13]. O. Laccourreye, A. Werner, J.P. Giroud, et al., Benefits, limits and danger of ephedrine and pseudoephedrine as nasal decongestants, *Eur. Ann. Otorhinolaryngol. Head Neck Dis.* 132 (2015) 31–34. DOI: 10.1016/j.anorl.2014.11.001

[14]. K. Głowacka, A. Wiela-Hojeńska, Pseudoephedrine – benefits and risks, *Int. J. Mol. Sci.* 22 (2021) 5146. DOI: 10.3390/ijms22105146

[15]. M. Weinberger, L. Hendeles, Theophylline in asthma, *N. Engl. J. Med.* 334 (1996) 1380–1388. DOI: 10.1056/NEJM199605233342107

[16]. T.S. Dnyanadev, M.N.A. Shete, N. Dnyaneshwari, et al., A review on: Ephedrine, *Pharmaceutical Resonance* 5 (2022) 6–8. https://pharmacy.dypvp.edu.in/pharmaceutical-resonance/downloads/original-research-articles/Volume-5-Issue-1/2.pdf

[17]. S.J. Stohs, M. Shara, S.D. Ray, p-Synephrine, ephedrine, p-octopamine and m-synephrine: Comparative mechanistic, physiological and pharmacological properties, *Phytother. Res.* 34 (2020) 1838–1846. DOI: 10.1002/ptr.6649

[18]. H.J. Yoo, H.Y. Yoon, J. Yee, et al., Effects of ephedrine-containing products on weight loss and lipid profiles: A systematic review and meta-analysis of randomized controlled trials, *Pharmaceuticals* 14 (2021) 1198. DOI: 10.3390/ph14111198

[19]. R.N. Chopra, B. Mukherjee, Toxic effects of ephedrine – a warning, *Ind. Med. Gaz.* 68 (1933) 622–626. PMCID: PMC5163782; PMID: 29009428

[20]. P. Rakovec, M. Kozak, M. Šebeštjen, Ventricular tachycardia induced by abuse of ephedrine in a young healthy woman, *Wien. Klin. Wochenschr.* 118 (2006) 558–561. DOI: 10.1007/s00508-006-0655-5

[21]. B.R. Matlaga, O.D. Shah, D.G. Assimos, Drug-induced urinary calculi, *Rev. Urol.* 5 (2003) 227–231. PMID: 16985842; PMCID: PMC1508366

[22]. G.M. Mekhova, A.N. Poskalenko, Effect of the new antidepressant cephedrine on compensatory hypertrophy of the ovaries and the inhibiting effect of estrogen, *Farmakol Toksikol.* 45 (1982) 52–54. PMID: 7056382

[23]. V.G. Pashinskiĭ, T.M. Vysokovskiĭ, Zh.N. Khlienko, et al., Toxicological properties of a cephedrine preparation, *Farmakol. Toksikol.* 41 (1978) 345–347. PMID: 658386

[24]. S. Fogel, Sudden death in asthma, *Can. Med. Assoc. J.* 114 (1976) 191. PMID: 1032350; PMCID: PMC1956924

[25]. B. Li, Z. Wang, Z. Liu, et al., DrugMetric: Quantitative drug-likeness scoring based on chemical space distance, *Briefings Bioinf.* 25 (2024) bbae321. DOI: 10.1093/bib/bbae321

[26]. W. Wei, S. Cherukupalli, L. Jing, et al., Fsp^3: A new parameter for drug-likeness, *Drug Discov. Today* 25 (2020) 1839–1845. DOI: 10.1016/j.drudis.2020.07.017

[27]. U. Fagerholm, S. Hellberg, J. Alvarsson, et al., Comparing Lipinski's rule of 5 and machine learning-based prediction of fraction absorbed for assessing oral absorption in humans, bioRxiv preprint (2024). DOI: 10.1101/2024.08.20.608791

[28]. T.W. Johnson, K.R. Dress, M. Edwards, Using the Golden Triangle to optimize clearance and oral absorption, *Bioorg. Med. Chem. Lett.* 19 (2009) 5560–5564. DOI: 10.1016/j.bmcl.2009.08.045

[29]. G. Falcón-Cano, C. Molina, M.Á. Cabrera-Pérez, Reliable prediction of Caco-2 permeability by supervised recursive machine learning approaches, *Pharmaceutics* 14 (2022) 1998. DOI: 10.3390/pharmaceutics14101998

[30]. P. Shah, V.B. Siramshetty, E. Mathé, X. Xu, Developing robust human liver microsomal stability prediction models: Leveraging inter-species correlation with rat data, *Pharmaceutics* 16 (2024) 1257. DOI: 10.3390/pharmaceutics16101257

[31]. A. Faris, I. Cacciatore, R. Alnajjar, et al., Computational insights into rational design and virtual screening of pyrazolopyrimidine derivatives targeting Janus kinase 3 (JAK3), *Front. Chem.* 12 (2024) 1425220. DOI: 10.3389/fchem.2024.1425220

[32]. M. Ríos-Gutiérrez, A. Saz Sousa, L.R. Domingo, Electrophilicity and nucleophilicity scales at different DFT computational levels, *J. Phys. Org. Chem.* 36 (2023) e4503. DOI: 10.1002/poc.4503

[33]. V. Yu, A. Ten, L. Baktybayeva, et al., Synthesis and biological evaluation of 1,3,8-triazaspiro[4.5]decane-2,4-dione derivatives as myelostimulators, *J. Chem.* 2018 (2018) 7346835. DOI: 10.1155/2018/7346835